

# Retrieval Augmented Generation for Dynamic Graph Modeling

**Yuxia Wu, Yuan Fang, Lizi Liao**

Singapore Management University

yieshah2017@gmail.com, yfang@smu.edu.sg, lzliaoj@smu.edu.sg

## Abstract

Dynamic graph modeling is crucial for analyzing evolving patterns in various applications. Existing approaches often integrate graph neural networks with temporal modules or redefine dynamic graph modeling as a generative sequence task. However, these methods typically rely on isolated historical contexts of the target nodes from a narrow perspective, neglecting occurrences of similar patterns or relevant cases associated with other nodes. In this work, we introduce the Retrieval-Augmented Generation for Dynamic Graph Modeling (RAG4DyG) framework, which leverages guidance from contextually and temporally analogous examples to broaden the perspective of each node. This approach presents two critical challenges: (1) How to identify and retrieve high-quality demonstrations that are contextually and temporally analogous to dynamic graph samples? (2) How can these demonstrations be effectively integrated to improve dynamic graph modeling? To address these challenges, we propose RAG4DyG, which enriches the understanding of historical contexts by retrieving and learning from contextually and temporally pertinent demonstrations. Specifically, we employ a time- and context-aware contrastive learning module to identify and retrieve relevant cases for each query sequence. Moreover, we design a graph fusion strategy to integrate the retrieved cases, thereby augmenting the inherent historical contexts for improved prediction. Extensive experiments on real-world datasets across different domains demonstrate the effectiveness of RAG4DyG for dynamic graph modeling.

## 1 Introduction

Dynamic graphs, which track the temporal evolution of nodes and edges, are essential for analyzing complex systems across domains like social networks, citation networks etc. Existing methods for dynamic graph modeling fall into two main categories: discrete-time and continuous-time approaches (Feng et al. 2024). Discrete-time methods divide the timeline into intervals, capturing the graph’s state at each point (Sankar et al. 2020), but they lack temporal granularity by overlooking event dynamics within intervals. Continuous-time approaches, on the other hand, model temporal dynamics continuously, without discretization, allowing for more detailed representations (Trivedi et al. 2019; Xu et al. 2020; Wen and Fang 2022). Our work aligns with continuous-time approaches, aiming to capture fine-grained time steps for more accurate dynamic graph modeling.

Traditional approaches for dynamic graph modeling predominantly rely on integrating graph neural networks (GNNs) with specialized temporal modules, such as recurrent neural networks (Pareja et al. 2020), self-attention (Sankar et al. 2020) and temporal point processes (Wen and Fang 2022), which update the graph representations over time. Although powerful, these methods suffer from the inherent limitations of GNNs, such as difficulty with long-term dependencies, and over-smoothing or over-squashing issues (Chen et al. 2020; Alon and Yahav 2020). Recently, a simple and effective approach called SimpleDyG (Wu, Fang, and Liao 2024) redefines dynamic graph modeling as a generative sequence modeling task and leverages the strengths of sequence models like Transformers to capture long-range dependencies within temporal sequences effectively.

Despite significant advancements in dynamic graph modeling, current approaches heavily depend on isolated historical contexts of the target nodes, limiting each node’s perspective to its ego network. The limited context makes it difficult to quickly adapt to diverse emerging patterns. For example, in a social network, when users transit to new behavioral patterns or when new users with minimal historical interactions are introduced, traditional models that focus on the historical contexts of individual nodes might not respond effectively to these changes. To overcome these limitations, we draw inspiration from the Retrieval-Augmented Generation (RAG) technique originated from the Natural Language Processing (NLP) field (Gao et al. 2023). As shown in Fig. 1(a), RAG broadens the context through the retrieval of additional demonstrations, achieving considerable success in NLP. In this work, we aim to integrate RAG into dynamic graph modeling to incorporate a broader and more relevant contextual understanding beyond the historical interactions of individual nodes. However, leveraging RAG for dynamic graph modeling presents two critical challenges.

First, *how do we harvest high-quality demonstrations for dynamic graphs?* This involves selecting the most contextually and temporally relevant samples to enrich the current state of a target node. Unlike RAG for NLP, where external textual data and a pre-trained language model (LM) naturally support demonstration retrieval as shown in Fig. 1(a), dynamic graph modeling requires careful consideration of the data sources and the ability to handle complex structural and temporal patterns as shown in Fig. 1(b). To address this,

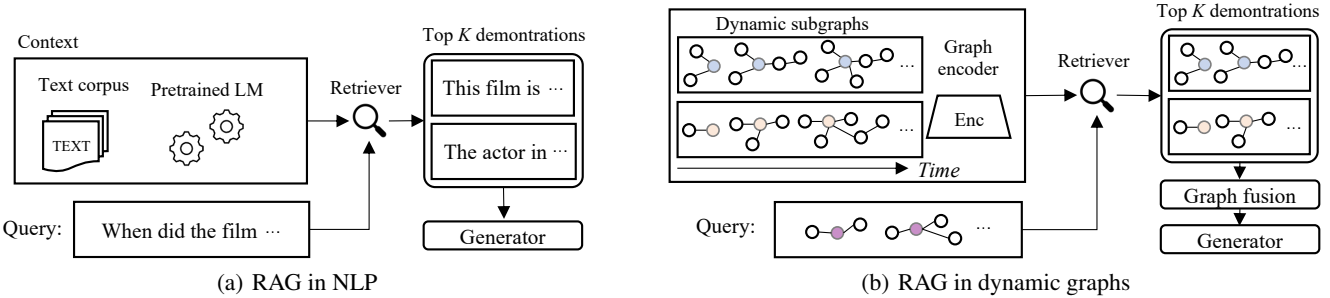


Figure 1: Illustration of RAG in NLP and dynamic graph modeling. (a) In NLP, RAG leverages pre-trained language models to encode text and retrieve semantically similar or related demonstrations, which are further concatenated to enhance the generation task. (b) Our work addresses the challenges of complex temporal and structural characteristics of dynamic graphs, incorporating RAG through time- and context-aware retrieval and graph fusion modules.

we introduce a novel time-aware contrastive learning strategy that leverages internal training data for demonstration retrieval. Following SimpleDyG (Wu, Fang, and Liao 2024), we regard dynamic graph modeling as a sequence modeling task and the prediction of future events as a sequence generation problem. Hence, we define a *query sequence* for a target node as its historical interaction sequence. Next, we automatically annotate the retrieval training pool by assessing the similarity to the query. Given the training pool, our model consists of two contrastive modules: time-aware and context-aware contrastive learning. The former utilizes a time decay function to prioritize samples that are temporally close to the query, while the latter incorporates data augmentation techniques such as masking and cropping to improve the model’s ability to retrieve complex structural patterns.

Second, *how do we effectively integrate the retrieved demonstrations into the dynamic graph model?* This involves fusing the retrieved demonstrations to enrich the historical context of each target node and enhance subsequent predictions. Directly concatenating the retrieved demonstrations with the query sequence not only results in a lengthy sequence unsuited for generative predictions but also overlooks the structural patterns among the retrieved demonstrations. To address this, we propose graph fusion, leveraging the graph structures inherent to the demonstrations and fusing them into a summary graph, as shown in Fig. 1(b). We then apply a GNN-based readout to learn the representation of the fused summary graph, which is prepended to the query sequence before being fed into the sequence generation model.

Our contributions can be summarized as follows. (1) We propose a novel Retrieval-Augmented Generation approach for Dynamic Graph modeling named RAG4DyG. It employs a retriever to broaden the historical interactions with contextually and temporally relevant demonstrations, leading to enhanced generative predictions on dynamic graphs. (2) We propose a time-aware contrastive learning module that incorporates temporal and structural information for demonstration retrieval. Additionally, we design a graph fusion module to effectively integrate the retrieved demonstrations, leveraging structural enhancements for subsequent predictions. (3) We conduct extensive experiments to validate our

approach, demonstrating the effectiveness of RAG4DyG in various domains.

## 2 Related Work

**Dynamic Graph Modeling.** Existing approaches for dynamic graphs can be categorized into discrete-time and continuous-time methods. Discrete-time methods regard a dynamic graph as a sequence of static graph snapshots captured at various time steps. Each snapshot represents the graph structure at a specific time step. These methods typically adopt GNNs to model the structural information of each snapshot, and then incorporate a sequence model (Pareja et al. 2020; Sankar et al. 2020) to capture the changes across snapshots. However, these approaches neglect fine-grained time information within a snapshot. In contrast, continuous-time methods model graph evolution as a continuous process, capturing all time steps for more precise temporal modeling. These methods often integrate GNNs with specially designed temporal modules, such as temporal random walk (Wang et al. 2021), temporal graph attention (Xu et al. 2020; Rossi et al. 2020), MLP-mixer (Cong et al. 2022) and temporal point processes (Trivedi et al. 2019; Ji et al. 2021; Wen and Fang 2022). Recently, researchers have proposed a simple and effective architecture called SimpleDyG (Wu, Fang, and Liao 2024), which reformulates the dynamic graph modeling as a sequence modeling task. Specifically, it maps the dynamic graph into a series of node sequences and feeds them into a generative sequence model. Subsequently, predicting future events can be framed as a sequence generation problem.

**Retrieval Augmented Generation.** Recently, the RAG paradigm has attracted increasing attention (Gao et al. 2023). Specifically, RAG first leverages the retriever to search and extract relevant documents from some databases, which then serve as additional context to enhance the generation process. Related studies have demonstrated the great potential of RAG in various tasks such as language processing (Karpukhin et al. 2020; Jiang et al. 2023), recommendation systems (Ye et al. 2022; Dao et al. 2024), and computer vision (Liu et al. 2023; Kim et al. 2024).

In the graph modeling field, existing RAG efforts have

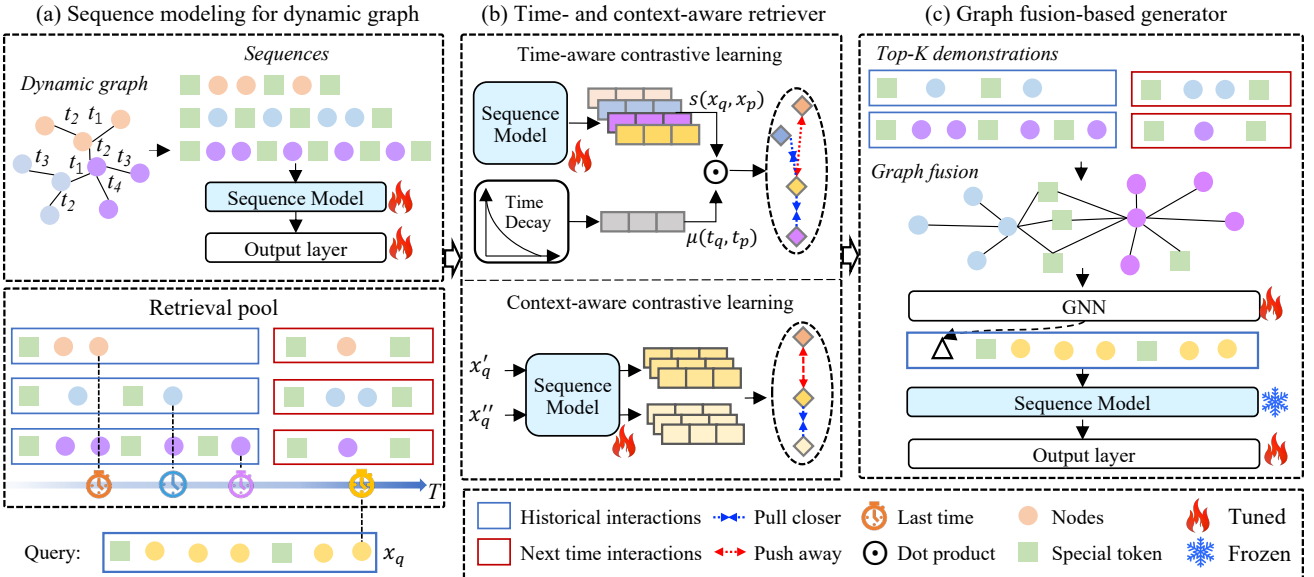


Figure 2: Overall framework of RAG4DyG. (a) Sequence modeling for dynamic graphs. (b) The retriever finds top- $K$  temporally and contextually relevant demonstrations. (c) Graph fusion integrates the retrieved demonstrations for subsequent generation.

primarily focused on static and text-attributed graphs to enhance the generation capabilities of Large Language Models, supporting graph-related tasks such as code summarization (Liu et al. 2021) and textual graph question answering (He et al. 2024; Hu et al. 2024). However, exploiting RAG techniques for dynamic graphs and graphs without textual information remains largely unexplored.

### 3 Preliminaries

In this section, we introduce the sequence modeling of dynamic graphs and the problem formulation.

**Sequence Mapping of Dynamic Graphs.** We denote a dynamic graph as  $G = (V, E, F, \mathcal{T})$  comprising a set of nodes  $V$ , edges  $E$ , a node feature matrix  $F$  if available, and a time domain  $\mathcal{T}$ . To map a dynamic graph into sequences, we follow SimpleDyG (Wu, Fang, and Liao 2024). Specifically, let  $D = \{(x_i, y_i)\}_{i=1}^M$  denote the set of training samples, where each sample is a pair  $(x_i, y_i)$ , representing the input and output sequences for a target node  $v_i \in V$ . The input  $x_i$  is a chronologically ordered sequence of nodes that have historically interacted with  $v_i$ , while the output  $y_i$  is the ground truth interactions that occurs following the sequence  $x_i$ . In notations, we have

$$x_i = [\text{hist}], v_i, [\text{time\_}1], v_i^{1,1}, v_i^{1,2}, \dots, [\text{time\_}t], v_i^{t,1}, \dots, [\text{time\_}T], v_i^{T,1}, \dots, [\text{eohist}], \quad (1)$$

$$y_i = [\text{pred}], [\text{time\_}T+1], v_i^{T+1,1}, \dots, [\text{eopred}], \quad (2)$$

where  $[\text{hist}]$ ,  $[\text{eohist}]$ ,  $[\text{pred}]$ ,  $[\text{eopred}]$  are special tokens denoting the input and output sequence, and  $[\text{time\_}1], \dots, [\text{time\_}T+1]$  are special time tokens representing different time steps.

**Problem Formulation.** Dynamic graph modeling aims to learn a model that can predict the future interactions of a

target node  $v_i$ , given its historical interactions. That is, given  $x_i$  in Eq. (1), the task is to predict  $y_i$  in Eq. (2).

In our RAG framework, we regard the training samples  $D$  as a retrieval pool. Given a target node  $v_q \in V$ , its input sequence  $x_q$  is referred to as the *query sequence*. We first retrieve  $K$  demonstrations  $R_q = \{(x_k, y_k)\}_{k=1}^K$  for each query sequence  $x_q$  based on their contextual and temporal relevance. Next, the retrieved demonstrations  $R_q$  are used to enrich the input sequence  $x_q$ , which encompasses the historical interactions of the target node  $v_q$ . The augmented input  $\{R_q, x_q\}$  is designed to enhance the predictions of future events in  $y_q$ .

### 4 Proposed Model: RAG4DyG

Our proposed RAG4DyG framework, depicted in Fig. 2, first trains a generative sequence model for dynamic graphs in Fig. 2(a). We use SimpleDyG (Wu, Fang, and Liao 2024) as the backbone for this task. As described in Sect. 3, a dynamic graph  $G$  is represented as sequences of node interaction records, which are then used to train a Transformer-based sequence model.

Next, given a query sequence  $x_q$  and a retrieval pool  $D$ , a time- and context-aware retriever is designed to retrieve demonstrations for  $x_q$  from  $D$ , as shown in Fig. 2(b). The retriever fine-tunes its encoder (*i.e.*, the sequence model) to jointly optimize two contrastive losses: a time-aware loss that employs a time decay function, and a context-aware loss that employs sequence augmentation. (Sect. 4.1)

Finally, given top- $K$  demonstrations retrieved from the retrieval pool, we design a graph fusion module as illustrated in Fig. 2(c). Specifically, we fuse the  $K$  demonstrations into a summary graph, leveraging the graph structures inherent to the retrieved demonstrations. The summary graph is further encoded by a GNN, serving as an augmented context that is prepended to the original query sequence. The augmented

sequence is subsequently input to the sequence model to predict future events. (Sect. 4.2)

#### 4.1 Time- and Context-Aware Retriever

Unlike NLP retrievers, dynamic graph retrieval requires consideration of temporal proximity alongside contextual relevance. To address this, we propose a time- and context-aware retrieval model with two contrastive learning modules. First, we incorporate a time decay mechanism to account for temporal proximity between query and candidate sequences. Second, we use sequence augmentation to capture intrinsic contextual patterns.

**Retrieval Annotation.** To facilitate contrastive training, we automatically annotate the samples in the retrieval pool  $D$ . For each query sequence  $x_q$ , we annotate its positive sample  $x_p^+$  from the pool  $D$  based on their contextual similarity. Specifically, we adopt the sequence model pre-trained in Fig. 2(a) as the encoder and apply mean pooling to obtain sequence representations. Given a query sequence  $x_q$  and a candidate sequence  $x_p \in D$ , we define their contextual similarity as the dot product of their representations:

$$s(x_q, x_p) = f(x_q)^\top f(x_p), \quad (3)$$

where  $f(\cdot)$  denotes our encoder. We leave the detailed annotation process in Appendix A.

**Time-aware Contrastive Learning.** Temporal information reflects the dynamic changes in historical interactions, which is crucial for dynamic graph modeling. We posit that demonstrations closer in time to the query are more relevant than those further away. Consequently, we utilize a time decay function to account for temporal proximity between the query and candidate sequences, as follows.

$$\mu(t_q, t_p) = \exp(-\lambda|t_q - t_p|), \quad (4)$$

where  $t_q$  and  $t_p$  represent the last interaction time in the query and candidate sequences<sup>1</sup>, respectively. The hyper-parameter  $\lambda$  controls the rate of time decay, determining how quickly the importance of interactions decreases with time. Note that  $0 < \mu(\cdot, \cdot) \leq 1$ . By using this time decay function, we assign higher importance to the candidates that are temporally closer to the query.

To effectively capture the temporal dynamics of the graph, we incorporates temporal proximity to reweigh the contextual similarity in the contrastive loss:

$$h(x_q, x_p) = s(x_q, x_p)\mu(t_q, t_p). \quad (5)$$

Subsequently, we adopt in-batch negative sampling based on the following training objective:

$$\mathcal{L}_{\text{tcl}} = -\log \frac{\exp(h(x_q, x_p^+))/\tau}{\sum_{j=1}^{2N} \mathbb{1}_{j \neq q} \exp(h(x_q, x_j))/\tau}, \quad (6)$$

where  $x_p^+$  denotes the positive sample of  $x_q$ ,  $N$  is the batch size, and  $\tau$  is the temperature parameter.

<sup>1</sup>In the annotated training data, the query time  $t_q$  may precede the candidate time  $t_p$ . However, in the validation and test sets,  $t_p$  always precedes  $t_q$ , preventing leakage from a future time.

**Context-aware Contrastive Learning.** To better capture the inherent contextual pattern, we further adopt context-aware contrastive learning with data augmentations. For each sequence, we apply two types of augmentations: masking and cropping, which are widely used for sequence modeling (Devlin et al. 2019; Xie et al. 2022). The masking operator randomly replaces a portion of the tokens in the sequence with a special masking token. The cropping operator randomly deletes a contiguous subsequence from the original sequence, reducing the sequence length while preserving the temporal order of the interactions. These augmentations help the model learn robust representations and capture the inherent structural information of the sequence by focusing on its different parts.

We treat two augmented views of the same sequence as positive pairs, and those of different sequences as negative pairs. Given a sequence  $x_q$  and its two distinct augmented views  $x_q'$  and  $x_q''$ , the contrastive loss is defined as:

$$\mathcal{L}_{\text{ccl}} = -\log \frac{\exp(s(x_q', x_q'')/\tau)}{\sum_{j=1}^{2N} \mathbb{1}_{j \neq q} \exp(s(x_q', x_j')/\tau)}, \quad (7)$$

where  $\tau$  is the temperature,  $N$  is the batch size and  $\mathbb{1}$  is an indicator function.

**Training and Inference for Retrieval.** The training objective of our retrieval model is defined as:

$$\mathcal{L}_{\text{ret}} = \mathcal{L}_{\text{tcl}} + \alpha \mathcal{L}_{\text{ccl}} \quad (8)$$

where  $\alpha$  is a coefficient that controls the balance between the two losses.

During testing, we utilize the updated sequence model to extract sequence representations and perform demonstration ranking based on the contextual similarity between the query and candidates.

#### 4.2 Graph Fusion-based Generator

After retrieval, we obtain the top- $K$  demonstrations  $R_q = \{(x_k, y_k)\}_{k=1}^K$  for the query  $x_q$ . A straightforward approach is concatenating them with the query sequence. However, this can lead to a lengthy context that limits the model’s prediction capabilities. More importantly, it neglects the structural patterns among these demonstrations. Thus, we first fuse the demonstrations into a summary graph, process it using a GNN, and then prepend the graph readout from the GNN to the query for subsequent generation.

**Graph Fusion.** To effectively fuse the demonstrations in  $R_q$ , we construct a summary graph, whose nodes include all tokens in the retrieved demonstrations, and edges represent the interactions between nodes within each sequence. Considering that there are common tokens across the retrieved demonstrations (e.g., recurring nodes in multiple demonstrations and special tokens like `[hist]`, `[time1]`, etc.), we can fuse these demonstrations into a summary graph  $G_{\text{fus}}$ . We then employ a graph convolutional network (GCN) to capture the structural and contextual information within the fused graph, and apply a mean-pooling readout to obtain a representation

Dataset	UCI	Hept	MMConv
Domain	Social	Citation	Conversation
# Nodes	1,781	4,737	7,415
# Edges	16,743	14,831	91,986

Table 1: Dataset statistics.

vector for the graph. The vector is subsequently concatenated with the query sequence representation, as follows.

$$e_{\text{fus}} = \text{MeanPooling}(\text{GCN}(G_{\text{fus}})), \quad (9)$$

$$\tilde{x}_q = [e_{\text{fus}} \parallel x_q], \quad (10)$$

where  $e_{\text{fus}}$  is the fused graph representation, and  $\tilde{x}_q$  is the retrieval-augmented sequence. The augmented sequence is fed into the sequence model, which generates future interactions.

**Training and inference.** We adopt the same sequence model with the same training objective (Wu, Fang, and Liao 2024) as in Fig. 2(a). During training, we freeze the parameters of the sequence model, except for the output layer which is updated along with the GCN parameters used for graph fusion.

During testing, we first apply the retriever model to retrieve top- $K$  demonstrations for each query as introduced in Sect. 4.1. Then we perform graph fusion on these demonstrations and concatenate the fused graph representation with the query sequence as illustrated in Eqs. (9) and (10). The concatenated sequence is subsequently fed into the trained sequence model for link prediction.

## 5 Experiment

In this section, we empirically evaluate the proposed model RAG4DyG compared to state-of-the-art methods and conduct a detailed analysis of the performance.

### 5.1 Experimental Setup

**Datasets.** We evaluate the performance of the proposed model on three datasets from different domains including the communication network UCI (Panzarasa, Opsahl, and Carley 2009), the citation network Hept (Leskovec, Kleinberg, and Faloutsos 2005), and the multi-turn task-oriented conversation dataset MMConv (Liao et al. 2021). We follow the same dataset preprocessing as SimpleDyG (Wu, Fang, and Liao 2024). It is important to note that the ML-10M dataset was not used because it is not suitable for RAG; we observed no performance enhancement even when the query was augmented with ground-truth demonstrations. We summarize the statistics of the three datasets in Table 1.

**Baselines.** We compare RAG4DyG with the state-of-the-art approaches of dynamic graph modeling. (1) discrete-time approaches: DySAT (Sankar et al. 2020) and EvolveGCN (Pareja et al. 2020); (2) continuous-time approaches: DyRep (Trivedi et al. 2019), JODIE (Kumar, Zhang, and Leskovec 2019), TGAT (Xu et al. 2020), TGN (Rossi et al. 2020), TREND (Wen and Fang 2022), GraphMixer (Cong et al. 2022) and SimpleDyG (Wu, Fang, and Liao 2024). The details of the baselines can be found in Appendix B.

**Implementation Details.** Following the method outlined in (Cong et al. 2022; Wu, Fang, and Liao 2024), we represent the dynamic graph as an undirected graph. We split all datasets into training, validation, and test sets based on temporal sequence same as SimpleDyG (Wu, Fang, and Liao 2024). Given  $T$  timesteps in each dataset, the data at the final timestep  $T$  is used as the testing set, the data at  $T - 1$  is served as the validation set, and the remaining data from earlier timesteps is used for training. All training data including the retrieval pool for the retriever and generator is drawn from this training data split. For retrieval augmented generation model training, we first train SimpleDyG without augmentation using the reported parameter in this paper. Then we fix the parameters of SimpleDyG except for the last linear layer and fine-tune them with the GCN model. The number of GCN layers in the generator model is 1 for all datasets. We repeat each experiment 10 times and report the average results along with the standard deviation. The number of demonstrations is 7 for all datasets. Hyper-parameter tuning is performed on the validation set and we provide the settings in Appendix D.

**Evaluation Metrics.** We evaluate the performance upon three metrics Recall@5, NDCG@5 and Jaccard (Wu, Fang, and Liao 2024). Recall@5 and NDCG@5 are widely used in ranking tasks measuring the quality of top-ranked predictions (Wang et al. 2019). Recall@5 assesses the proportion of relevant nodes in the top 5 predictions, while NDCG@5 evaluates the ranking quality by considering the positions of the relevant nodes. Jaccard (Jaccard 1901) measures the similarity between the predicted and ground truth sequences by comparing the intersection and union of the two sets.

### 5.2 Performance Comparison

We evaluate the performance of RAG4DyG for the dynamic link prediction task, and the results compared to the state-of-the-art baselines are presented in Table 2. We make the following observations.

The proposed RAG4DyG generally outperforms all baselines across different datasets under the three metrics. In particular, compared to SimpleDyG, which is also our backbone, RAG4DyG consistently shows superior performance, highlighting the effectiveness of our retrieval-augmented generation framework. Note that GraphMixer performs slightly better in Recall@5 on the MMConv dataset, but its significantly lower performance in NDCG@5 and Jaccard indicates that its predictions are not ranked optimally or maintaining the overall set integrity compared to RAG4DyG. This indicates that RAG4DyG can better model the temporal and contextual relationships due to the specific design of the retriever and generator.

Second, RAG4DyG exhibits significant advantages in inductive scenarios such as the Hept dataset. This setting is particularly challenging because it involves nodes not appearing during the training phase, requiring the model to generalize to entirely new structures and relationships. RAG4DyG's success is attributed to its retrieval-augmented mechanism, which enhances the model's ability to generalize by providing rich contextual information relevant to the

Method	UCI			Hept			MMConv		
	Recall@5	NDCG@5	Jaccard	Recall@5	NDCG@5	Jaccard	Recall@5	NDCG@5	Jaccard
DySAT	0.009±0.003	0.010±0.003	0.010±0.001	0.008±0.004	0.007±0.002	0.005±0.001	0.108±0.089	0.102±0.085	0.095±0.080
EvolveGCN	0.072±0.046	0.064±0.045	0.032±0.026	0.008±0.002	0.009±0.004	0.007±0.002	0.050±0.015	0.051±0.021	0.032±0.017
DyRep	0.009±0.008	0.011±0.018	0.010±0.005	0.009±0.006	0.031±0.024	0.010±0.006	0.156±0.054	0.140±0.057	0.067±0.025
JODIE	0.018±0.019	0.022±0.023	0.012±0.009	0.010±0.008	0.031±0.021	0.011±0.008	0.052±0.039	0.041±0.016	0.032±0.022
TGAT	0.022±0.004	0.061±0.007	0.020±0.002	0.011±0.007	0.034±0.023	0.011±0.006	0.118±0.004	0.089±0.033	0.058±0.021
TGN	0.014±0.010	0.041±0.017	0.011±0.003	0.011±0.006	0.030±0.012	0.008±0.001	0.085±0.050	0.096±0.068	0.066±0.038
TREND	0.083±0.015	0.067±0.010	0.039±0.020	0.010±0.008	0.031±0.003	0.010±0.002	0.134±0.030	0.116±0.020	0.060±0.018
GraphMixer	0.097±0.019	<u>0.104±0.013</u>	0.042±0.005	0.009±0.002	0.011±0.008	0.010±0.003	<b>0.206±0.001</b>	0.172±0.029	0.085±0.016
SimpleDyG	0.109±0.014	<u>0.104±0.010</u>	<u>0.092±0.014</u>	0.013±0.006	0.035±0.014	<u>0.013±0.006</u>	0.170±0.010	0.184±0.012	<u>0.169±0.010</u>
RAG4DyG	<b>0.111±0.013</b>	<b>0.122±0.014</b>	<b>0.097±0.010</b>	<b>0.019±0.002</b>	<b>0.045±0.003</b>	<b>0.019±0.002</b>	<u>0.194±0.005</u>	<b>0.208±0.005</b>	<b>0.194±0.005</b>

Table 2: Performance comparison for dynamic link prediction. (Best results are bolded; runners-up are underlined.)

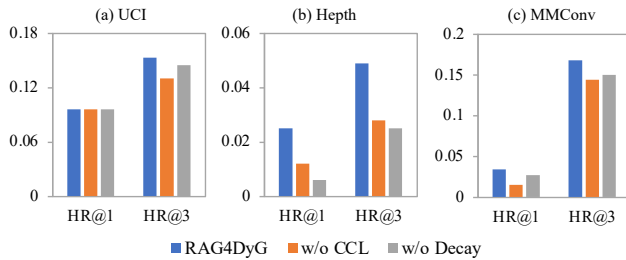


Figure 3: Ablation study for retrieval results.

new, unseen nodes. Unlike models that rely solely on the immediate neighborhood or predefined structures, RAG4DyG dynamically adapts to the new nodes, ensuring that the predictions are guided by the most relevant and similar historical data.

### 5.3 Model Analysis

We analyze the behavior of our model RAG4DyG in several aspects, including an ablation study, an investigation of the effectiveness of different retrieval methods, and an analysis of parameter sensitivity.

**Ablation Study.** To evaluate the effectiveness of different modules in the retrieval model, we compare RAG4DyG with two variants *w/o CCL* and *w/o Decay* which exclude the context-aware contrastive learning and time decay component in the retrieval model. We evaluate the performance for both retrieval and link prediction tasks. We use  $HR@k$  (Hit Ratio@ $k$ ) metrics for the retrieval model, measuring the proportion of cases where at least one of the top- $k$  retrieved items is relevant. As shown in Fig. 3 and 4, the full model outperforms the two variants, underscoring the benefits of incorporating context-aware contrastive learning and time decay modulation.

**Effect of Different Retrieval Methods.** To further investigate the effectiveness of the retrieval model, we compare our model with two different retrieval methods, namely, BM25 and Jaccard, in Table 3 and 4. In Table 4, we only report NDCG@5 and present the remaining metrics in Appendix C. BM25 (Fang, Tao, and Zhai 2004) is an extension

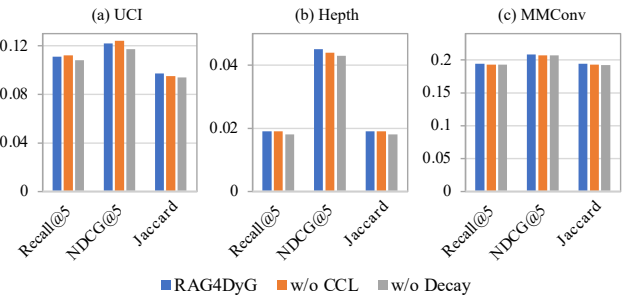


Figure 4: Ablation study for link prediction results.

of the Term Frequency-Inverse Document Frequency (TF-IDF) model, which calculates a relevance score between the query sequence and each candidate sequence in the retrieval pool. The relevance score is derived from the occurrence frequency of the nodes in the query and the retrieval pool. Jaccard (Jaccard 1901) measures the similarity between two sets by comparing the size of their intersection to the size of their union. Note that in the citation dataset Hept, all queries in the test set only contain unseen target nodes that never appear in the retrieval pool and have no historical interactions. As a result, the BM25 and Jaccard scores between the queries and the candidates in the retrieval pool are always zeros. On the other hand, our retrieval model is trained based on the sequence representations. For a query sequence containing only the target node, we can still obtain its representation using the sequence model trained for the retrieval model, and further calculate its contextual similarity with the candidate sequences in the retrieval pool.

In Table 3, we analyze the retrieval performance of different retrieval methods. Our retrieval model shows better performance than other retrieval strategies. Notably, in inductive scenarios like the Hept dataset, BM25 and Jaccard fail to work with new query nodes lacking historical interactions. In contrast, our model can handle them effectively and achieve solid performance. The high  $HR@3$  performance of BM25 and Jaccard on the MMConv dataset can be attributed to the nature of the dialogue dataset, where temporal order is less critical, and certain nodes associated with specific slot

Method	UCI		Hepth		MMConv	
	HR@1	HR@3	HR@1	HR@3	HR@1	HR@3
<i>BM25</i>	<b>0.100</b>	0.136	-	-	0.025	<b>0.233</b>
<i>Jaccard</i>	<b>0.100</b>	0.109	-	-	0.007	0.213
<i>RAG4DyG</i>	0.096	<b>0.153</b>	<b>0.025</b>	<b>0.049</b>	<b>0.034</b>	0.168

“-” denotes that the method is unable to perform retrieval. The reason is explained in the corresponding description of this table in Sect. 5.3.

Table 3: Retrieval performance of various retrieval methods.

Method	UCI	Hepth	MMConv
<i>BM25</i>	0.121±0.009	-	0.207±0.003
<i>Jaccard</i>	0.113±0.011	-	0.207±0.005
<i>RAG4DyG</i>	<b>0.122±0.014</b>	<b>0.045±0.003</b>	<b>0.208±0.005</b>
<i>GroundTruth</i>	0.129±0.010	0.062±0.007	0.224±0.008

See the note in Table 3 for the explanation of “-”.

Table 4: Generative accuracy of various retrieval methods.

values are more discriminative.

Table 4 shows the generative performance of different retrieval methods in the dynamic link prediction task. During testing, we apply the retrieval results obtained from different retrieval methods. We also train a model using the ground-truth retrieval results for a more comprehensive comparison. The “GroundTruth” row represents an upper bound on the performance when using ground-truth retrieval results on the testing data, which, as expected, provides the highest performance metrics. Generally speaking, all retrieval methods show better performance compared to the backbone SimpleDyG without using RAG, demonstrating the effectiveness of the RAG technique for dynamic graph modeling. Our method performs better compared to other retrieval strategies, indicating the effectiveness of contrastive learning in the retrieval model.

**Effect of the Number of Demonstrations  $K$ .** To investigate the influence of the number of demonstrations, we conduct experiments across varying values  $K \in \{1, 3, 5, 7, 9\}$ . As shown in Fig. 5, a higher number of  $K$  yields better prediction performance, that’s because more demonstrations provide richer contextual information, especially in the UCI dataset. However, including too many cases may introduce more noise, which can harm the performance.

**Effect of Different Fusion Strategies.** To further investigate the effectiveness of the fusion strategy for the top- $K$  demonstrations, we conduct experiments with different fusion strategies in Table 5 for  $K = 7$ . We report NDCG@5 in Table 4 and present the other metrics in Appendix C. “Concatenation” denotes we directly concatenate the sequences of retrieved demonstrations and prepend them with the query sample sequence and then feed it into the pre-trained SimpleDyG model. “MLP” means we do not consider the graph structure of the demonstrations and replace the graph fusion as an MLP layer (we set the number of the MLP layer as 2). By using the MLP layer, We map the concatenated demon-

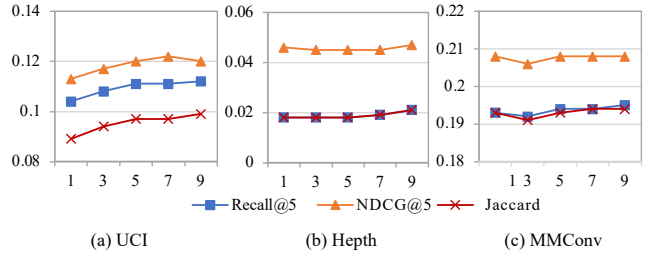


Figure 5: Effect of the number of demonstrations  $K$ .

Fusion strategy	UCI	Hepth	MMConv
<i>Concatenation</i>	0.036±0.018	0.007±0.002	0.110±0.030
<i>MLP</i>	0.106±0.017	0.015±0.002	0.167±0.006
<i>GraphFusion</i>	<b>0.122±0.014</b>	<b>0.045±0.003</b>	<b>0.208±0.005</b>

Table 5: Effect of different fusion strategies.

strations into shorter  $m$ -dimensional embeddings (we empirically set  $m$  to be 15) and then concatenate it with the query sample. Like graph fusion, we only fine-tune the parameters of the MLP and output layer. The results in Table 5 show that directly concatenating the retrieved demonstrations with the query sample leads to lower performance compared with other strategies. This is because simple concatenation introduces a lengthy context, which can overwhelm the model with irrelevant information, and it neglects the structural relationships inherent in the demonstrations. The “MLP” strategy improves upon this by mapping the concatenated demonstrations into a shorter feature space, effectively reducing noise and emphasizing more relevant features. This approach yields better results than simple concatenation but still falls short compared to the “GraphFusion” strategy. The superior performance of the “GraphFusion” strategy highlights the importance of considering both the content and the structure of the demonstrations in the fusion process.

## 6 Conclusion

In this work, we introduced a novel retrieval augmented framework RAG4DyG for dynamic graph modeling, addressing the limitations of existing approaches that often rely on narrow historical contexts. We leverage the RAG technique to broaden the context by incorporating relevant auxiliary information by harvesting high-quality demonstrations for dynamic graph samples and effectively utilizing this demonstration to enhance dynamic graph modeling. Our proposed solution involves a time-aware contrastive learning model to identify and retrieve temporally pertinent cases for each query sequence, coupled with a graph fusion strategy to integrate the inherent historical context with extended temporal contexts. Extensive experiments on real-world datasets across different domains demonstrated the superior performance of RAG4DyG in dynamic graph modeling.

## References

Alon, U.; and Yahav, E. 2020. On the Bottleneck of Graph Neural Networks and its Practical Implications. In *International Conference on Learning Representations*.

Chen, D.; Lin, Y.; Li, W.; Li, P.; Zhou, J.; and Sun, X. 2020. Measuring and relieving the over-smoothing problem for graph neural networks from the topological view. In *Proceedings of the AAAI conference on artificial intelligence*, volume 34, 3438–3445.

Cong, W.; Zhang, S.; Kang, J.; Yuan, B.; Wu, H.; Zhou, X.; Tong, H.; and Mahdavi, M. 2022. Do We Really Need Complicated Model Architectures For Temporal Networks? In *The Eleventh International Conference on Learning Representations*.

Dao, H.; Deng, Y.; Le, D. D.; and Liao, L. 2024. Broadening the View: Demonstration-augmented Prompt Learning for Conversational Recommendation. In *Proceedings of the 47th International ACM SIGIR Conference on Research and Development in Information Retrieval*, 785–795.

Devlin, J.; Chang, M.-W.; Lee, K.; and Toutanova, K. 2019. BERT: Pre-training of Deep Bidirectional Transformers for Language Understanding. In *Proceedings of the 2019 Conference of the North American Chapter of the Association for Computational Linguistics: Human Language Technologies, Volume 1 (Long and Short Papers)*, 4171–4186.

Fang, H.; Tao, T.; and Zhai, C. 2004. A formal study of information retrieval heuristics. In *Proceedings of the 27th annual international ACM SIGIR conference on Research and development in information retrieval*, 49–56.

Feng, Z.; Wang, R.; Wang, T.; Song, M.; Wu, S.; and He, S. 2024. A Comprehensive Survey of Dynamic Graph Neural Networks: Models, Frameworks, Benchmarks, Experiments and Challenges. *arXiv preprint arXiv:2405.00476*.

Gao, Y.; Xiong, Y.; Gao, X.; Jia, K.; Pan, J.; Bi, Y.; Dai, Y.; Sun, J.; and Wang, H. 2023. Retrieval-augmented generation for large language models: A survey. *arXiv preprint arXiv:2312.10997*.

He, X.; Tian, Y.; Sun, Y.; Chawla, N. V.; Laurent, T.; LeCun, Y.; Bresson, X.; and Hooi, B. 2024. G-retriever: Retrieval-augmented generation for textual graph understanding and question answering. *arXiv preprint arXiv:2402.07630*.

Hu, Y.; Lei, Z.; Zhang, Z.; Pan, B.; Ling, C.; and Zhao, L. 2024. GRAG: Graph Retrieval-Augmented Generation. *arXiv preprint arXiv:2405.16506*.

Jaccard, P. 1901. Étude comparative de la distribution florale dans une portion des Alpes et des Jura. *Bull Soc Vaudoise Sci Nat*, 37: 547–579.

Ji, Y.; Jia, T.; Fang, Y.; and Shi, C. 2021. Dynamic heterogeneous graph embedding via heterogeneous hawkes process. In *Machine Learning and Knowledge Discovery in Databases. Research Track: European Conference, ECML PKDD 2021, Bilbao, Spain, September 13–17, 2021, Proceedings, Part I 21*, 388–403. Springer.

Jiang, Z.; Xu, F. F.; Gao, L.; Sun, Z.; Liu, Q.; Dwivedi-Yu, J.; Yang, Y.; Callan, J.; and Neubig, G. 2023. Active Retrieval Augmented Generation. In *Proceedings of the 2023 Conference on Empirical Methods in Natural Language Processing*, 7969–7992.

Karpukhin, V.; Oguz, B.; Min, S.; Lewis, P.; Wu, L.; Edunov, S.; Chen, D.; and Yih, W.-t. 2020. Dense Passage Retrieval for Open-Domain Question Answering. In *Proceedings of the 2020 Conference on Empirical Methods in Natural Language Processing (EMNLP)*, 6769–6781.

Kim, J.; Cho, E.; Kim, S.; and Kim, H. J. 2024. Retrieval-Augmented Open-Vocabulary Object Detection. In *Proceedings of the IEEE/CVF Conference on Computer Vision and Pattern Recognition*, 17427–17436.

Kumar, S.; Zhang, X.; and Leskovec, J. 2019. Predicting dynamic embedding trajectory in temporal interaction networks. In *Proceedings of the 25th ACM SIGKDD international conference on knowledge discovery & data mining*, 1269–1278.

Leskovec, J.; Kleinberg, J.; and Faloutsos, C. 2005. Graphs over time: densification laws, shrinking diameters and possible explanations. In *Proceedings of the eleventh ACM SIGKDD international conference on Knowledge discovery in data mining*, 177–187.

Liao, L.; Long, L. H.; Zhang, Z.; Huang, M.; and Chua, T.-S. 2021. MMConv: an environment for multimodal conversational search across multiple domains. In *Proceedings of the 44th international ACM SIGIR conference on research and development in information retrieval*, 675–684.

Liu, H.; Son, K.; Yang, J.; Liu, C.; Gao, J.; Lee, Y. J.; and Li, C. 2023. Learning customized visual models with retrieval-augmented knowledge. In *Proceedings of the IEEE/CVF Conference on Computer Vision and Pattern Recognition*, 15148–15158.

Liu, S.; Chen, Y.; Xie, X.; Siow, J. K.; and Liu, Y. 2021. Retrieval-Augmented Generation for Code Summarization via Hybrid GNN. In *International Conference on Learning Representations*.

Panzarasa, P.; Opsahl, T.; and Carley, K. M. 2009. Patterns and dynamics of users’ behavior and interaction: Network analysis of an online community. *Journal of the American Society for Information Science and Technology*, 60(5): 911–932.

Pareja, A.; Domeniconi, G.; Chen, J.; Ma, T.; Suzumura, T.; Kanezashi, H.; Kaler, T.; Schardl, T.; and Leiserson, C. 2020. Evolvegen: Evolving graph convolutional networks for dynamic graphs. In *Proceedings of the AAAI conference on artificial intelligence*, volume 34, 5363–5370.

Rossi, E.; Chamberlain, B.; Frasca, F.; Eynard, D.; Monti, F.; and Bronstein, M. 2020. Temporal graph networks for deep learning on dynamic graphs. *arXiv preprint arXiv:2006.10637*.

Sankar, A.; Wu, Y.; Gou, L.; Zhang, W.; and Yang, H. 2020. Dysat: Deep neural representation learning on dynamic graphs via self-attention networks. In *Proceedings of the 13th international conference on web search and data mining*, 519–527.

Trivedi, R.; Farajtabar, M.; Biswal, P.; and Zha, H. 2019. Dyrep: Learning representations over dynamic graphs. In *International conference on learning representations*.

Wang, X.; He, X.; Wang, M.; Feng, F.; and Chua, T.-S. 2019. Neural graph collaborative filtering. In *Proceedings of the 42nd international ACM SIGIR conference on Research and development in Information Retrieval*, 165–174.

Wang, Y.; Chang, Y.-Y.; Liu, Y.; Leskovec, J.; and Li, P. 2021. Inductive Representation Learning in Temporal Networks via Causal Anonymous Walks. In *International Conference on Learning Representations (ICLR)*.

Wen, Z.; and Fang, Y. 2022. Trend: Temporal event and node dynamics for graph representation learning. In *Proceedings of the ACM Web Conference 2022*, 1159–1169.

Wu, Y.; Fang, Y.; and Liao, L. 2024. On the Feasibility of Simple Transformer for Dynamic Graph Modeling. In *Proceedings of the ACM on Web Conference 2024*, 870–880.

Xie, X.; Sun, F.; Liu, Z.; Wu, S.; Gao, J.; Zhang, J.; Ding, B.; and Cui, B. 2022. Contrastive learning for sequential recommendation. In *2022 IEEE 38th international conference on data engineering (ICDE)*, 1259–1273. IEEE.

Xu, D.; Ruan, C.; Korpeoglu, E.; Kumar, S.; and Achan, K. 2020. Inductive representation learning on temporal graphs.

Ye, C.; Liao, L.; Liu, S.; and Chua, T.-S. 2022. Reflecting on experiences for response generation. In *Proceedings of the 30th ACM International Conference on Multimedia*, 5265–5273.

## Appendix

### A Retrieval Data Annotation

To facilitate retrieval model training, we regard the samples in the training dataset as our retrieval pool  $D = \{(x_i, y_i)\}_{i=1}^M$  where each pair  $(x_i, y_i)$  represents the historical sequence and its corresponding target sequence. Specifically,  $x_i$  is the input sequence before the last time step and  $y_i$  is the output sequence at the last time step. We annotate demonstrations based on the Jaccard similarity of  $y_i$  among all the pairs in  $D$ .

$$r(y_i, y_j) = \frac{|y_i \cap y_j|}{|y_i \cup y_j|} \quad (11)$$

To control the quality of annotated data, we set a threshold of 0.8 to select highly similar demonstrations for each sample. These filtered annotations are then used to train the retriever model. The number of training samples for UCI, Hept and MMConv datasets are 9,578, 8,250 and 10,762, respectively.

### B More Details about Baselines

The details of the baselines are as follows:

- **DySAT** (Sankar et al. 2020) utilizes self-attention mechanisms to capture both structural and temporal patterns in dynamic graphs through discrete-time snapshots.
- **EvolveGCN** (Pareja et al. 2020) leverages recurrent neural networks to evolve the graph convolutional network parameters over discrete time steps.
- **DyRep** (Trivedi et al. 2019) models dynamic graphs in continuous time by incorporating both temporal point processes and structural dynamics to capture interactions and node dynamics.
- **JODIE** (Kumar, Zhang, and Leskovec 2019) focuses on user and item embedding trajectories over continuous time, predicting future interactions by modeling user and item embeddings jointly.
- **TGAT** (Xu et al. 2020) employs temporal graph attention layers and time encoding to capture temporal dependencies and structural information for dynamic graphs.
- **TGN** (Rossi et al. 2020) combines GNNs with memory modules to maintain node states over continuous time, effectively learning from dynamic interactions.
- **TREND** (Wen and Fang 2022) integrates temporal dependencies based on Hawkes process and GNN to learn the dynamics of graphs.
- **GraphMixer** (Cong et al. 2022) introduces a novel architecture that leverages MLP-mixer to learn link-encoder and node encoder for evolving graphs in continuous time.
- **SimpleDyG** (Wu, Fang, and Liao 2024) reformulated the dynamic graph modeling as a sequence modeling task and mapped the dynamic interactions of target nodes as sequences with specially designed tokens. It simplifies dynamic graph modeling without complex architectural changes to effectively capture temporal dynamics.

### C More Experimental Results

For the effect of different retrieval methods for generative performance in Sec. 5.3, we report the NDCG@5 score in Table 4. Here we report the remaining metrics in Table 6. The results show that RAG4DyG performs better than BM25 and Jaccard on Recall@5 and Jaccard metrics, which are consistent with the performance of NDCG@5.

Method	UCI		Hept		MMConv	
	Recall@5	Jaccard	Recall@5	Jaccard	Recall@5	Jaccard
BM25	0.111 $\pm$ 0.007	0.093 $\pm$ 0.004	-	-	0.193 $\pm$ 0.003	0.192 $\pm$ 0.003
Jaccard	0.104 $\pm$ 0.009	0.088 $\pm$ 0.010	-	-	0.193 $\pm$ 0.004	0.192 $\pm$ 0.004
RAG4DyG	0.111 $\pm$ 0.013	0.097 $\pm$ 0.010	0.019 $\pm$ 0.002	0.019 $\pm$ 0.002	0.194 $\pm$ 0.005	0.194 $\pm$ 0.005
GroundTruth	0.121 $\pm$ 0.010	0.107 $\pm$ 0.012	0.028 $\pm$ 0.004	0.028 $\pm$ 0.004	0.210 $\pm$ 0.008	0.208 $\pm$ 0.008

Table 6: Generative performance of retrieval methods.

For the effect of different fusion strategies in Sec. 5.3, the performance of the remaining metrics is shown in Table 7. Similarly, the “GraphFusion” strategy outperforms direct concatenation and “MLP”, indicating the effectiveness of the graph structure among demonstrations.

Fusion strategy	UCI		Hept		MMConv	
	Recall@5	Jaccard	Recall@5	Jaccard	Recall@5	Jaccard
Concatenation	0.033 $\pm$ 0.019	0.029 $\pm$ 0.016	0.001 $\pm$ 0.002	0.002 $\pm$ 0.002	0.103 $\pm$ 0.031	0.103 $\pm$ 0.031
MLP	0.102 $\pm$ 0.018	0.089 $\pm$ 0.016	0.006 $\pm$ 0.002	0.006 $\pm$ 0.002	0.156 $\pm$ 0.006	0.153 $\pm$ 0.006
GraphFusion	0.111 $\pm$ 0.013	0.097 $\pm$ 0.010	0.019 $\pm$ 0.002	0.019 $\pm$ 0.002	0.194 $\pm$ 0.005	0.194 $\pm$ 0.005

Table 7: Effect of different fusion strategies.

### D Hyper-parameter Settings

We run all the experiments on an NVIDIA GPU L40 with the same data splitting and follow the hyper-parameter settings reported in SimpleDyG (Wu, Fang, and Liao 2024) for all the baselines. For our RAG4DyG method, we report the hyper-parameters as follows.

The time decay rate  $\lambda$  for the retrieval model in Eq. (4) was fine-tuned according to the time granularity of different datasets, with days for the UCI dataset, months for the Hept dataset, and turns for the MMConv dataset. We explored a range of values  $\lambda = \{1e-4, 1e-3, 1e-2, 1e-1, 1, 10, 100\}$ , ultimately selecting  $\lambda = 1e-4$  for UCI,  $\lambda = 0.1$  for Hept, and  $\lambda = 10$  for MMConv. The coefficient  $\alpha$  in the loss function (Eq. (8)) was tuned across  $\{0.2, 0.4, 0.6, 0.8, 1\}$ , resulting in final values of  $\alpha = 1$  for UCI and MMConv dataset,  $\alpha = 0.4$  for Hept. Additional parameter settings for the three datasets are as follows: the temperature  $\tau$  in the two contrastive learning tasks is set to  $\tau = \{0.1, 0.1, 0.1\}$ ; the batch size of the retriever model is  $N = \{64, 128, 128\}$ ; and the masking and cropping portions in context-aware contrastive learning are  $\{0.8, 0.8, 0.8\}$  and  $\{0.4, 0.6, 0.6\}$ , respectively.